Transactions, SMiRT-24
BEXCO, Busan, Korea - August 20-25, 2017
Division II

VALIDATION OF DEFECT SIZE TO BE DETECTED DURING ISI BASED ON PROBABILISTIC FRACTURE MECHANICS

Masaki Nagai[1], Naoki Miura[2], Hajime Shohji[3], and Yasukazu Takada[4]

[1] Research Scientist, Central Research Institute of Electric Power Industry, Japan
[2] Associate Vice President, Central Research Institute of Electric Power Industry, Japan
[3] Senior Research Scientist, Central Research Institute of Electric Power Industry, Japan
[4] Manager, The Kansai Electric Power Company, Incorporated, Japan

ABSTRACT

In nuclear power plants, when cracks are detected in piping during in-service inspection (ISI), structural integrity assessment is required to be conducted on the basis of fitness-for-service codes. Detection and sizing of such cracks with high accuracy are necessary for reliable flaw evaluation, which plays an important role in the structural integrity of piping. Ultrasonic testing (UT) is a widely applied technique for ISI. In Japan, sizing accuracy of a crack detected in the weld of austenitic stainless steel piping is assured by the Performance Demonstration system. Regarding detection capability, discussion on the confirmation of the detection skill of UT engineers through an appropriate training is being held at the Japan Electric Association. The depth of the crack, which trainees are required to detect in order to complete the training, should be evaluated based on structural integrity evaluation. Probabilistic fracture mechanics (PFM) is focused on as the convincing method for structural integrity evaluation in a rational manner.

In this paper, the probability of detection (POD) curve was expressed by using the following two parameters: One is the minimum detectable crack depth and the other is the certainly detectable crack depth corresponding to the POD of 100%. PFM analysis code taking into account this POD curve was developed. Then we performed several PFM analyses with different parameter sets of POD curve. Consequently, the effect of the crack depth with POD of 100% on the leak probability was more significant than that of the minimum detectable crack depth.

INTRODUCTION

Ultrasonic testing (UT) is a widely applied technique for in-service inspection (ISI) of components in nuclear power plants (NPPs). When cracks are detected in piping during ISI, structural integrity assessment is required to be conducted on the basis of fitness-for-service codes such as JSME Rules on Fitness-for-Service for Nuclear Power Plants (2012). Detection and sizing of such cracks with high accuracy are necessary for reliable flaw evaluation, which plays an important role in the structural integrity of piping. In Japan, UT for ISI has been performed by certified UT engineers with a great deal of experience (2008). Furthermore, performance demonstration (PD) system (2015), such as PDI programs, is currently only applied to crack depth sizing on the weld of austenitic stainless steel piping. On the other hand, discussions on training system and guidelines are being held at the Japan Electric Association (JEA) in order to improve the reliability of detection capability. In developing the guideline, the detection capability required for UT examination personnel who have completed the training program, for instance, crack depth to detected, should be evaluated based on the structural integrity. Probabilistic fracture mechanics (PFM) is focused on as the convincing method for structural integrity evaluation in a rational manner.

In this paper, the effect of the detection capability of UT engineers on the structural integrity of the weld of austenitic stainless steel piping was evaluated based on PFM analysis.

EVALUATION METHOD

Evaluation Specimen

For the purpose of training and education of UT engineers, who are engaged in the ISI of the weld of austenitic stainless steel piping, the use of the following specimens has been discussed:

(a) Piping for boiling water reactor (BWR) plants
- Specimen with nominal diameter of 100A and thickness of 8.6 mm
- Specimen with nominal diameter of 600A and thickness of 39 mm
- Medium sized specimen, as an example, specimen with nominal diameter of 350A and thickness of 25 mm.

(b) Piping for pressurized water reactor (PWR) plants
- Specimen with nominal diameter of 50A and thickness of 8.7 mm
- Specimen with nominal diameter of 350A and thickness of 35.7 mm
- Medium sized specimen, as an example, specimen with nominal diameter of 250A and thickness of 25.4 mm

In Japan, most of flaws detected in the weld of austenitic stainless steel piping were found in BWR plants. In this paper, therefore, we focused on piping for BWR plants. These piping are assumed to be used for primary loop recirculation (PLR) system and cracks detected in the weld of PLR piping are supposed to be attributed to stress corrosion cracking (SCC). Because we considered that tendency can be seen by evaluating the former two of three specimens with different sizes, the medium sized specimen was not evaluated. According to Japan Industrial Standard (JIS), outer diameters of 100A and 600A were set to be 609.6 mm and 114.3 mm, respectively.

Evaluation Flow

In the evaluation of PFM, a circumferential semi-elliptical crack was postulated on inner surface of a pipe, and SCC crack propagation analysis and fracture analysis based on the net-section collapse criterion were performed by using the PEDESTRIAN (2016). A SCC crack was assumed to be existed at the start point of evaluation time, and crack initiation was not considered. We assumed that a pipe was replaced or repaired when a defect was detected by pre-service inspection (PSI) or ISI, which was conducted every ten years. PFM evaluation flow is shown in Figure 1.

Probability of Detection Curve

In order to carry out PFM analysis taking into account the detection capability of UT engineers, we implemented the probability of detection (POD) curve, which shows variation of the probability of detection depending on the crack depth. Harris, et al (1981) have proposed the POD curve for piping as follows:

$$POD = 1 - P_{ND} = 1 - \frac{1}{2}\mathrm{erfc}\left[\nu \ln\left(\frac{a}{a^*}\right)\right] \tag{1}$$

where P_{ND}, a and a^* are the probability of nondetection, the crack depth and the crack depth for 50% P_{ND}, respectively. ν is the parameter that controls the slope of the $P_{ND} - a$ curve. Backer, et al. (2001) evaluated the POD curve, which is represented by equation (1), for UT engineers based on actual UT data. The curve evaluated by Backer, et al. shows an unrealistic one that the probability of detection is greater than 0% even when the crack depth is 0 mm.

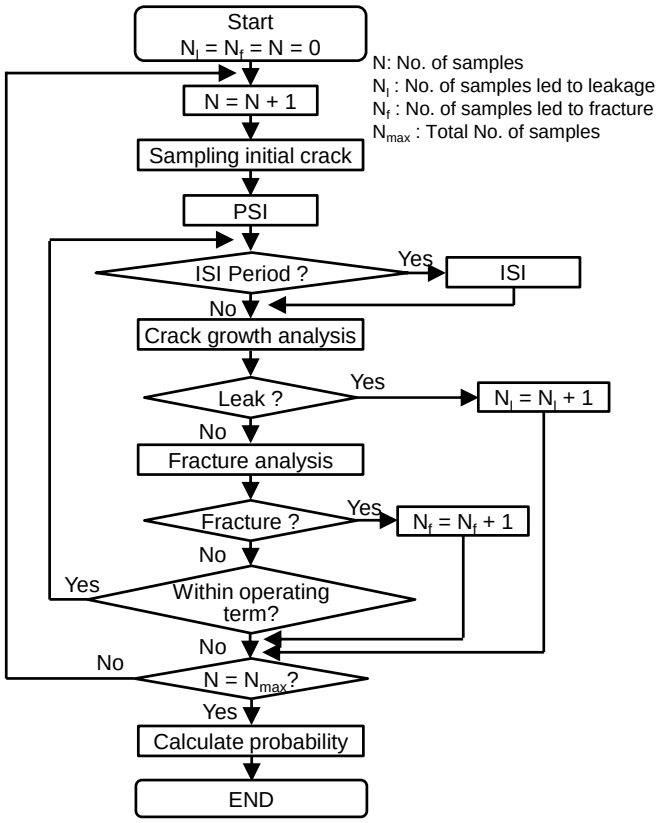

Figure 1 Evaluation flowchart

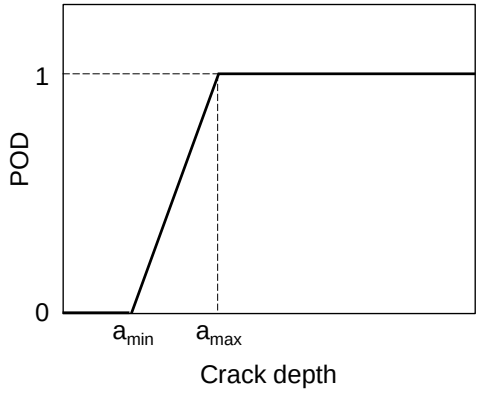

Figure 2 POD curve expressed by linear interpolation between a_{min} and a_{max}

In this study, the POD curve is expressed simply by the linear interpolation between the following two parameters: One is minimum detectable crack depth (a_{min}) and the other is the certainly detectable crack depth corresponding to 100% POD (a_{max}). Figure 2 shows the POD curve used in this paper. Herein, a_{min} and a_{max} are set to be 1 mm and 4 mm, respectively, as a standard condition. The value of a_{min} was decided taking into account realistic minimum detectable crack depth denoted in the earlier study (2010), and the value of a_{max} was determined to envelop the minimum depth of defects detected with the probability of 100%, which was obtained from the UT results for austenitic stainless steel piping performed by Japan Nuclear Energy Safety Organization (2005).

PFM Evaluation with POD Curve

In the PFM analysis code used in this study, a crack with certain depth was considered as a sample and the failure probability is calculated by the number of samples led to failure divided by total number of samples. In the case where PFM analysis is performed with taking into account PSI or ISI, the number of samples led to failure are multiplied by the probability of nondetection before the calculation of the failure probability. For instance, when inspections are performed at the time of pre-service, 5 years, 15 years, and 25 years after start of service, and the probabilities of nondetection at these times are 1, 0.9, 0.8, and 0.5, then the number of samples used in the calculation of the failure probability is obtained by 1 x 0.9 x 0.8 x 0.5.

Random Variables

In this section, random variables, which are summarized in Table 1, used in PFM analyses are described in detail.

Table 1 Random variables used in this paper

Variables	Probability density function
Initial crack depth, a	(a) Exponential distribution $P_a(a) = \frac{e^{-a/\mu_a}}{\mu_a\left(1-e^{-h/\mu_a}\right)}$, μ_a = 6.248 mm (b) Normal distribution μ_a = 5.47 mm, σ_a = 2.17 mm
Initial crack aspect ratio, c/a	Log-normal distribution: $P_{c/a}(c/a) = \frac{1}{(c/a)\gamma\sqrt{2\pi}}\exp\left(-\frac{1}{2}\left\{\frac{\ln[(c/a)/\beta]}{\gamma}\right\}^2\right)$ α = 1.419, β = 1.336, γ = 0.5382
SCC crack growth rate $\frac{da}{dt} = CK^m$	C: Log-normal distribution <Heat Affected Zone> $\mu_{C\_HAZ} = 9.018\times10^{-11}$, σ_{C_HAZ} = 0.303, upper limit = 9.2×10^{-7} <Weld metal> $\mu_{C\_Weld} = 1.017\times10^{-11}$, σ_{C_Weld} = 1.120, upper limit = 2.1×10^{-7} m: Fixed 2.161
Distance from weld metal to a crack, L	Normal distribution μ_L = 1.15 mm, σ_L = 1.39 mm
Flow stress, σ_{fs}	Normal distribution μ_{fs} = 436.4 MPa, σ_{fs} = 46.2 MPa

1. Initial crack depth

Several probability density functions for initial crack depth have been proposed. In this paper, we used the following two distributions since the different types of probability density function could affect PFM result:

(i) Exponential distribution

$$P_a(a) = \frac{\exp(-a/\mu_a)}{\mu_a\left[1-\exp(-t/\mu_a)\right]} \tag{2}$$

where μ_a and t are mean value of the crack depth a and thickness, respectively. Harris, et al. (1981) set μ_a to 6.248 mm for primary piping of PWR plants and we used this value for PLR piping.

(ii) Normal distribution

$$P_a(a) = \frac{1}{\sigma_a\sqrt{2\pi}}\exp\left[-\frac{1}{2}\left(\frac{a-\mu_a}{\sigma_a}\right)^2\right] \tag{3}$$

where μ_a and σ_a are median and standard deviation of the crack depth a, respectively. Machida (2011) reported sizes of SCCs that were detected in the PLR piping in some Japanese BWR plants. Using these data, Machida provided μ_a = 5.47 mm and σ_a = 2.17 mm. Figure 3 (a) shows the initial crack depth distribution using equation (2) and (3) for pipe with the nominal diameter of 600A. Most of the crack depth data shown in Machida's report were detected in 600A pipe. Thus, the initial crack depth distribution of the pipe with the nominal diameter of 100A was determined as follows: It is widely known that initiation of SCC crack is affected by residual stress distribution. As described below, in this paper, we used the same residual stress distribution, which is normalized with regard to the thickness, of pipe with the nominal diameter of 100A as that of 600A pipe. The initial crack depth distribution, which is

normalized with regard to the thickness, of 100A pipe was assumed to be equal to that of 600A pipe in the same way as residual stress distribution. Figure 3 (b) shows the initial crack depth distribution of 100A pipe.

Herein, the normal distribution defined in equation (3) was obtained by the depth distribution of cracks detected in actual components. Therefore, it is considered that this distribution does not contain cracks whose depths are less than minimum detectable crack depth. On the other hand, considering that weld residual stress distribution shows a large tensile stress on the inner surface and compression stress in the centre of the thickness of the pipe, the exponential distribution that takes the maximum value on the inner surface seems to be close to actual distribution of the initial crack depth.

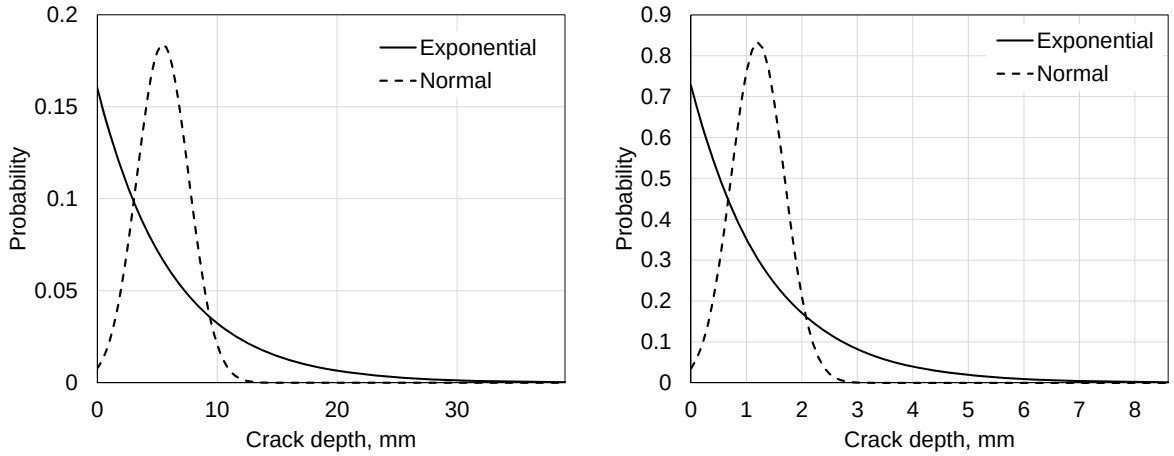

(a) 600A pipe (b) 100A pipe

Figure 3 Distribution of initial crack depth

2. Initial crack aspect ratio

Harris, et al (1981) pointed out that the length of deep crack was more likely to be longer than that of shallow crack. Therefore, assuming that the crack depth and the crack aspect ratio are independent is more reasonable than assuming that the depth and the surface length are independent. According to Harris' proposal, the following probability density function for the crack aspect ratio was used:

$$P_{c/a}(c/a) = \frac{1}{(c/a)\gamma\sqrt{2\pi}} \exp\left(-\frac{1}{2}\left\{ \frac{\ln\left[(c/a)/\beta\right]}{\gamma} \right\}^2 \right) \tag{4}$$

where α = 1.419, β = 1.336 and γ = 0.5832, which were shown in Harris' report, were used in this paper.

3. Flow stress

The probability density function of flow stress used in the fracture analysis based on the net-section collapse criterion was obtained by extracting the data of flow stress of SUS304 base metal at room temperature from the available data sheet (1997). The obtained 11 pieces of data provide μ_{fs} = 436.4 MPa and σ_{fs} = 46.2 MPa. The data quantity of the flow stress is not sufficient to represent the normal distribution. But other reliable data were not available, and therefore we used 11 pieces of data.

4. SCC crack growth rate

According to the document (2009), in the evaluation of SCC crack growth in the weld of PLR piping, the rate of the sensitized stainless steel was used in the heat affected zone (HAZ) and the rate of

stainless steel with low carbon content was used in the weld metal. These crack growth rates are expressed as follows:

$$\frac{da}{d\tau} = CK^m \tag{5}$$

where $da/d\tau$ is the crack growth rate, which has the unit of mm/s, and K is the stress intensity factor, which has the unit of MPa $m^{1/2}$. C and m are the material properties determined experimentally. In the Machida's report (2011), C was assumed to be random variable and its probabilistic density function was obtained as the following form by processing statistically the data, which were used to determine the SCC crack growth rate given in the JSME S-NA1-2012:

Median: $\mu_{C\_HAZ} = 9.018 \times 10^{-11}$, standard deviation: $\sigma_{C\_HAZ} = 0.303$ at HAZ
Median: $\mu_{C\_Weld} = 1.017 \times 10^{-11}$, standard deviation: $\sigma_{C\_Weld} = 1.120$ at weld metal

In this paper, C was treated as random variables based on the above values and m was treated as a constant value which was equal to 2.161. The upper limited values of crack growth rates were set to be the following values according to the JSME S-NA1-2012:

Upper limited rate = 9.2×10^{-7} mm/s at HAZ
Upper limited rate = 2.1×10^{-7} mm/s at weld metal

Figures 4(a) and 4(b) show SCC crack growth rate at HAZ portion and weld metal portion, respectively. These figures show that SCC crack growth rate at HAZ and weld metal given in JSME S-NA1-2012 are approximately 2σ and 1σ of available data, respectively. Leakage was considered to occur when a/t reached 0.75.

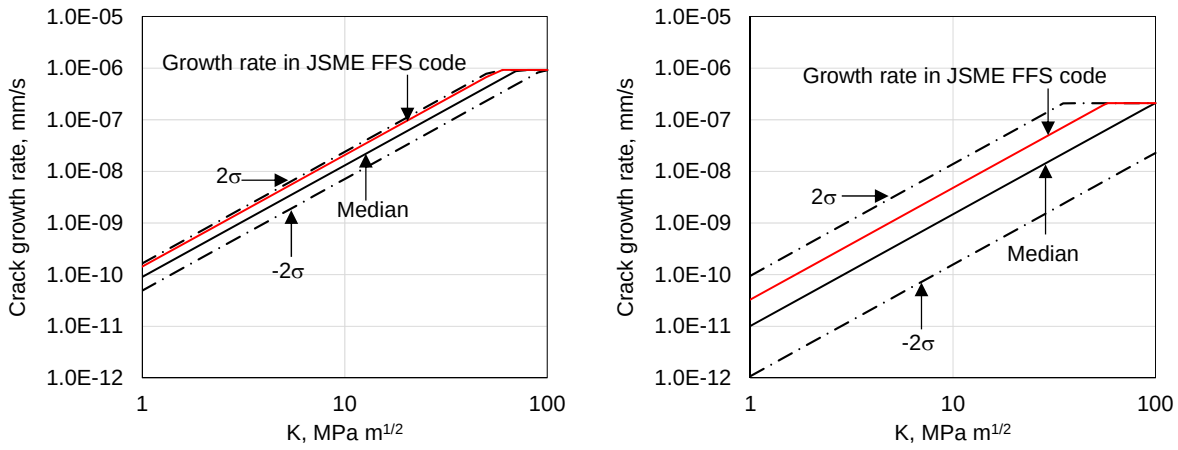

(a) HAZ portion (b) Weld metal portion

Figure 4 SCC crack growth rates

5. Distance between weld fusion line and SCC crack

According to the document (2009), the crack depth, d, at the time when a SCC crack initiated in the HAZ portion of PLR piping reaches the weld metal portion, is determined by the following equation:

$$d = 1.0L + 5.7 \tag{6}$$

where L is the distance between the weld fusion line and the initiation position of a SCC crack, as shown in figure 5. Machida (2011) processed statistically the data of SCC cracks that were detected in the PLR piping in some Japanese BWR plants and showed L as the normal distribution with the median of 1.15 mm and the standard deviation of 1.39 mm. In this analysis, we treated L as random variable described by the above normal distribution. The crack growth rate at the HAZ portion is used until the crack depth reaches d defined by equation (6). After the depth reaches d, the crack growth rate at the weld metal is applied. The data of d were obtained from the piping with the nominal diameter of 600A. Because other reliable data were not available for the piping with the nominal diameter of 100A, we applied d of 600A pipe to that of 100A pipe.

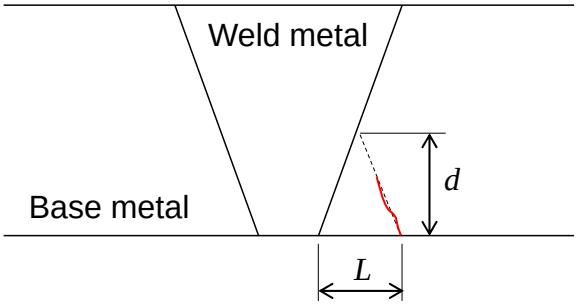

Figure 5 Distance between weld fusion line and crack

Table 2 Applied stress used in crack growth analysis

	Internal pressure p, MPa	Membrane stress P_m, MPa
100A(8.6t)	9.0	60.9
600A(39t)	9.0	60.9

Table 3 Applied stress used in fracture analysis

	Membrane stress P_m, MPa	Bending stress P_b, MPa
100A(8.6t)	32.9	28.0
600A(39t)	27.7	33.0

Applied Load Condition

In the applied load condition, weld residual stress and normal operation loads, which are internal pressure p, membrane stress P_m, and bending stress P_b caused by thermal expansion, were assumed. In this analysis, discharge-side pressure of 9 MPa for PLR pump was used as internal pressure p, which is applied on the inner surface of the crack in the evaluation of crack growth. In the SCC crack growth analysis, according to Miura's report (1998), $P_m = 0.5S_m$ and $P_b = 0$, where S_m stands for the design stress intensity and $S_m = 121.8$ MPa was used, were assumed. On the other hand, in the fracture analysis by the net-section collapse criterion, the value of P_m was calculated by using internal pressure $p = 9$ MPa and $P_b = 0.5S_m - P_m$ was applied because it is necessary to consider bending stress based on the JSME S-NA1-2012. Normal operation loads are summarized in Tables 2 and 3.

Residual stress distributions in the weld of PLR piping with the nominal diameter of 300A, 400A and 600A were given in the sixth order polynomial form by Machida (2011). In the PFM analysis code used in this study, the stress intensity factors were calculated from the solutions, which corresponds to third order polynomial stress distribution, described in the JSME S-NA1-2012. Thus, residual stress distribution expressed by sixth order polynomial equation was approximated by third order polynomial form expressed in the following equation:

$$\sigma\left(\frac{x}{t}\right) = 391.99 - 3644.5\left(\frac{x}{t}\right) + 6945.7\left(\frac{x}{t}\right)^2 - 3540.6\left(\frac{x}{t}\right)^3 \quad (7)$$

where x is the distance from the inner surface of the pipe. Figure 6 shows residual stress distributions, which are expressed by sixth order polynomial equations, for the piping with the nominal diameter of 300A, 400A and 600A. In this figure, distribution defined in equation (7) is also shown. From this figure, stress distribution along the thickness, maximum and minimum values of stress are similar with each other and independent of the nominal diameter. As we could not find residual stress distribution of the

pipe with the nominal diameter of 100A, we used the distribution expressed by equation (7) as the stress distribution of the pipe with 100A. Actually, it is expected that maximum and minimum values of residual stress for the pipe with 100A are smaller than those with 600A because the thickness of the pipe with 100A is thinner than that with 600A.

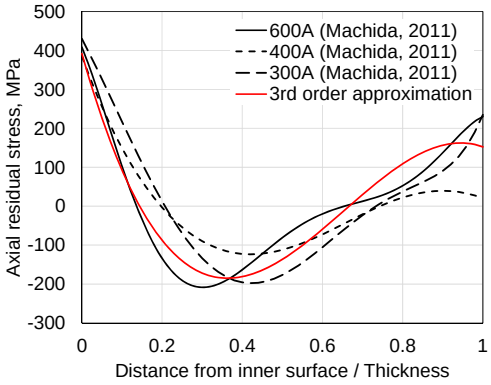

Figure 6 Weld residual stress distribution

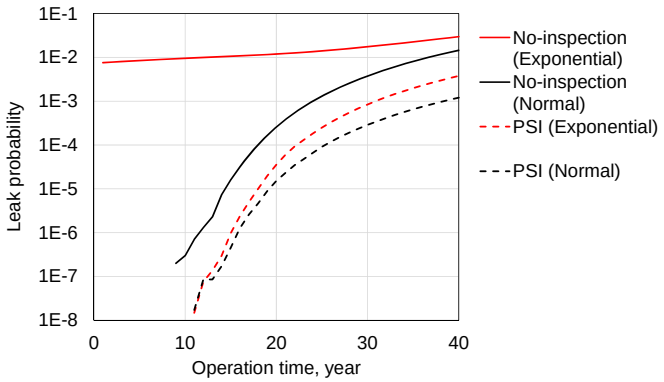

Figure 7 Effect of difference in distribution of initial crack depth on leak probability (600A pipe)

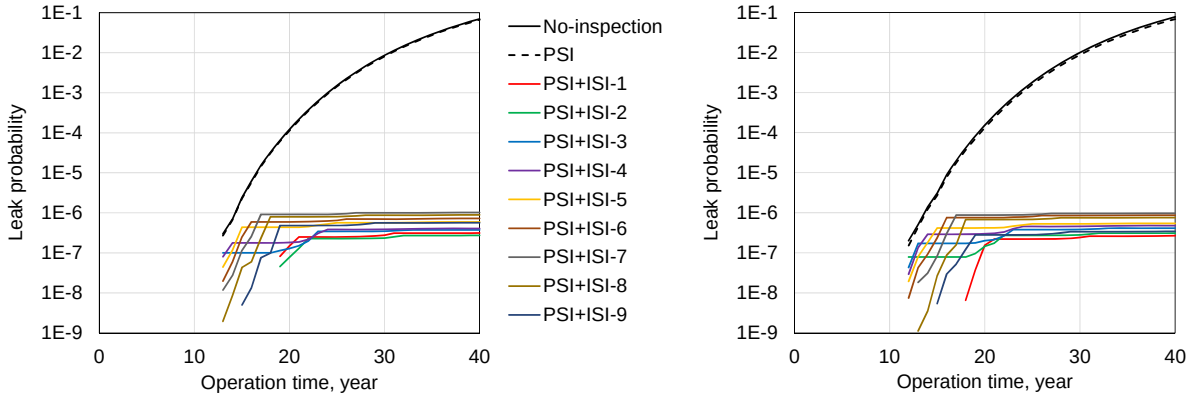

(a) Exponential distribution (b) Normal distribution

Figure 8 Effect of difference in ISI timing on leak probability (100A pipe)

EVALUATION RESULTS

PFM analyses were performed by using the conditions described above. The total number N of repeated analysis was set to be 10^7 in accordance with our previous study (2016). As a result, there was no sample led to failure in the fracture analysis based on the net-section collapse criterion and all samples led to failure were attributed to leakage after SCC crack growth. In this section, PFM analysis results are shown by dividing into the following two parts: The first part shows that the effect of timing to perform ISI and the difference in the initial crack depth distribution on the leak probability, and the other part shows that the effect of different parameter sets of POD curve on the leak probability.

Effect of Timing to Perform ISI or Distribution of Initial Crack Depth on Leakage

Figures 7 and 8 show transients of the leak probability with time for the piping with the nominal diameter of 600A and 100A, respectively. The results shown in these figures were obtained by using the exponential distribution and the normal distribution as the distribution of the initial crack depth. These

figures show the results under the conditions where inspection was not performed, only PSI was performed, and both PSI and ISI were performed. The term of "PSI + ISI - 1" shown in figures stands for that inspection was conducted at the times of pre-service, 1 year, 11 years, 21 years and 31 years after start of service. Figure 7 does not show the leak probabilities under the condition where both PSI and ISI were performed. This means that there is no sample led to the leakage within the total number $N = 10^7$ of repeated analysis. In the case of no inspection, the leak probability obtained by using the exponential distribution is higher than that by using the normal distribution in all operation times. This may be caused by that the initial cracks with depths greater than 10 mm are sampled frequently in the exponential distribution comparing with the normal distribution (see figure 3). The leak probabilities obtained under the condition where only PSI was conducted are an order of magnitude lower than those obtained under the condition of no inspection. This seems to be caused by that the initial cracks with depths greater than 4 mm were detected certainly through PSI.

On the other hand, regarding the 100A pipe shown in figure 8, there is little difference between the leak probabilities obtained with only PSI and those obtained without inspection. This may be caused by that few initial cracks with depths greater than 4 mm are sampled in the case of no inspection. When ISI was performed in addition to PSI, the leak probabilities are deduced. In the case where both PSI and ISI were conducted, the leak probabilities are plotted within the range between 10^{-7} and 10^{-6} without depending on the timing to perform ISI and the difference in the initial crack depth distribution. Therefore, when ISI is conducted every ten years, the effect of the timing to conduct ISI on the leak probability is small. And, there is little difference in the leak probability between the exponential distribution and the normal distribution.

Because the leak probabilities obtained for the 600A pipe under the condition where both PSI and ISI were conducted becomes 0 within the total number $N = 10^7$ of repeated analysis, only the results for the 100A pipe are presented in the following discussion. Moreover, as discussed above, it is considered that the exponential distribution is reasonable as actual distribution of the initial crack depth, and the effect of the timing to conduct ISI on the leak probability is small. Therefore the results obtained by using the exponential distribution and in the condition of "PSI + ISI - 5" are shown in the following.

Effect of POD Curve on Leakage

The transitions of the leak probability with time are shown in figures 9 and 10 when a_{min} and a_{max} were changed as shown in these figures. Figure 9 shows the results obtained by shifting a_{min} by 0.5 mm based on 1 mm and fixing a_{max} of 4 mm. From this figure, the effect of change of a_{min} on the leak probability is small. Figure 10 shows the results obtained by shifting a_{max} by 1 mm based on 4 mm and fixing a_{min} of 1 mm. The leak probability obtained by increasing a_{max} by 1 mm is two orders of magnitude larger than that obtained by setting a_{max} to be 4 mm. On the other hand, the leak probability obtained by decreasing a_{max} by 1 mm is an order of magnitude lower than that obtained by setting a_{max} to be 4 mm.

According to the above results, UT engineers, who are engaged in ISI, must aim to reduce not a_{min} but a_{max}. In other words, UT engineers are required to have the capability to detect large cracks certainly.

CONCLUSION

In this study, the effect of the detection capability of UT engineers on the structural integrity of the weld of austenitic stainless steel piping was evaluated based on PFM analysis. The POD curve was expressed simply by the linear interpolation between a_{min} and a_{max}. Then we performed several PFM analyses with different combinations of a_{min} and a_{max} in the POD curve. As a result, it was ascertained that UT engineers engaged in ISI must aim to reduce not the minimum detectable crack depth a_{min}, but the certainly detected crack depth, a_{max}.

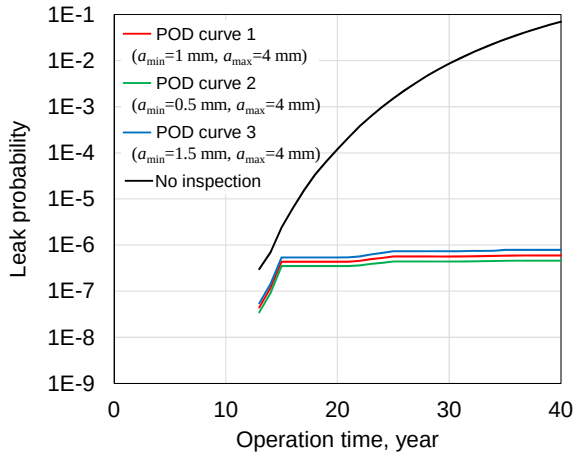

Figure 9 Effect of difference in a_{min} used in POD curve on leak probability

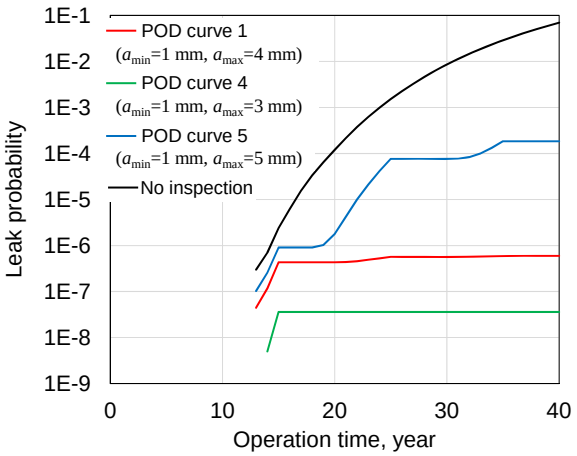

Figure 10 Effect of difference in a_{max} used in POD curve on leak probability

REFERENCES

Becker, F. L., "Performance Demonstration – 25 Years of Progress," Proceedings of 3rd International Conference of NDE in Relation to Structural Integrity for Nuclear and Pressurized Components, pp. 170-175, 2001.

Harris, D. O., Lim, E. Y. and Dedhia, D. D., "Probability of Pipe Fracture in the Primary Coolant Loop of a PWR Plant," NUREG/CR-2189, 1981.

Japan Electric Association, "Ultrasonic Examination for Inservice Inspection of Light Water Cooled Nuclear Power Plant Components," JEAC4207-2008, 2008.

Japan Nuclear Energy Safety Organization, "Report on nuclear power generation facility inspection technology demonstration project (related to defect detectability and sizing accuracy in ultrasonic flaw detection test), Synthesis report," 2005.

Japan Society of Mechanical Engineers, "Codes for Nuclear Power Generation Facilities, -Rules on Fitness-for-Service for Nuclear Power Plants-," JSME S-NA1-2012, 2012.

Machida, H., "Influence of Non-Destructive Examination Performance on Reliability of Pipes Having Stress Corrosion Cracks," Transactions of JSME, 77, pp. 1798-1813, 2011.

Ministry of Economy, Trade and Industry Nuclear and Industrial Safety Agency, "The interpretation of crack and other defects that cause a breakdown in the power generation nuclear power plant (internal rule)," 2009.

Miura N. and Chung, Y. K., "Effect of Combined Loading on Pipe Flaw Evaluation Criteria," CRIEPI report, T98015, 1998.

Nagai, M., Miura, N. and Yamamoto, M., "PEDESTRIAN: Probabilistic fracture mechanics analysis code based on sampling without replacement," *The 11th International Workshop on the Integrity of Nuclear Components 2016 (ASINCO-11)*, Nagasaki, Japan, April 2016.

Shimizu, K., et al. "Know-How for the Ultrasonic Examination Practice & Evaluation of PLR Piping," Maintenology, 8, pp. 31-36, 2010.

The Japan Society for Non-Destructive Inspection, "Qualification and certification of personnel for performance demonstration of ultrasonic testing systems", NDIS 0603, 2015.

USNRC, Pipe Fracture Encyclopedia, Volume 3, Pipe Fracture Test Data, 1997.